

This article was downloaded by: [University of Cambridge]

On: 15 September 2013, At: 15:00

Publisher: Taylor & Francis

Informa Ltd Registered in England and Wales Registered Number: 1072954

Registered office: Mortimer House, 37-41 Mortimer Street, London W1T 3JH, UK



Geophysical & Astrophysical Fluid Dynamics

Publication details, including instructions for authors and subscription information:

<http://www.tandfonline.com/loi/ggaf20>

Large and small scale motions in Kinematic dynamos

W. P. Wood^b & H. K. Moffatt^a

^a DAMTP, Silver Street, Cambridge, U. K.

^b Department of Mathematics, Statistics and Computer Science, University of Newcastle, New South Wales, 2308, Australia

Published online: 18 Aug 2006.

To cite this article: W. P. Wood & H. K. Moffatt (1985) Large and small scale motions in Kinematic dynamos, *Geophysical & Astrophysical Fluid Dynamics*, 32:2, 135-161

To link to this article: <http://dx.doi.org/10.1080/03091928508208782>

PLEASE SCROLL DOWN FOR ARTICLE

Taylor & Francis makes every effort to ensure the accuracy of all the information (the "Content") contained in the publications on our platform. However, Taylor & Francis, our agents, and our licensors make no representations or warranties whatsoever as to the accuracy, completeness, or suitability for any purpose of the Content. Any opinions and views expressed in this publication are the opinions and views of the authors, and are not the views of or endorsed by Taylor & Francis. The accuracy of the Content should not be relied upon and should be independently verified with primary sources of information. Taylor and Francis shall not be liable for any losses, actions, claims, proceedings, demands, costs, expenses, damages, and other liabilities whatsoever or howsoever caused arising directly or indirectly in connection with, in relation to or arising out of the use of the Content.

This article may be used for research, teaching, and private study purposes. Any substantial or systematic reproduction, redistribution, reselling, loan, sub-licensing, systematic supply, or distribution in any form to anyone is expressly forbidden. Terms & Conditions of access and use can be found at <http://www.tandfonline.com/page/terms-and-conditions>

Large and Small Scale Motions in Kinematic Dynamos

W. P. WOOD† and H. K. MOFFATT
DAMTP, Silver Street, Cambridge, U.K.

(Received July 24, 1984; in final form December 6, 1984)

Kinematic, axisymmetric mean field dynamos are examined for a number of models in order to study the cooperation between small scale turbulent motions (α -effect) and the large scale motions (ω -effect and meridional flow). For a spherical dynamo we show that it is more difficult to excite an α^2 -dynamo with dipolar parity in the presence of differential rotation, which increases with increasing depth, when the magnitude of the toroidal shearing effect is too small. Meridional streaming in the absence of differential rotation has an inhibitory effect on α^2 -dynamos. For dynamos in spheres the ease with which a dynamo is excited when the combined effects of differential rotation and meridional flow are present depends on the model for $\omega(r, \theta)$. For a model where the maximum in the toroidal shearing is towards the edge of the region enclosing the streamlines a small amount of meridional flow enhances dynamo action.

For dynamos confined to a spherical shell the effect of a small amount of single cell meridional flow is to enhance dynamo action when the toroidal shearing is confined to a narrow region near the lower boundary of the shell. If the shearing is located away from the boundary the meridional flow inhibits dynamo action. For speeds of flow considered here quadrupolar fields are more easily excited.

For circulation with a double cell structure dipolar oscillatory dynamos are more readily excited independent of the location of the maximum in the toroidal shearing effect.

†Permanent address: Department of Mathematics, Statistics and Computer Science, University of Newcastle, New South Wales, 2308, Australia.

1. INTRODUCTION

The theory of the turbulent dynamo provides a framework within which one attempts to account for various types of magnetic fields in cosmical bodies. Essentially two types of dynamo action are envisaged within the theory when it is considered in its simplest form. Either the magnetic field is produced by turbulent motions alone and these turbulent motions are parameterized by means of the α -effect (α^2 -dynamos) or else there is the combined effect of turbulent motion and differential rotation (the ω -effect) giving rise to an $\alpha\omega$ -dynamo. In the literature (e.g. Moffatt, 1978; Krause and Rädler, 1980) the steady fields characteristic of α^2 -dynamos have normally been associated with the earth's magnetic field while the $\alpha\omega$ -dynamos have been invoked to model many of the properties of the solar field.

A number of numerical studies (Roberts, 1972; Roberts and Stix, 1972; Jepps, 1975 and Rädler, 1975) have been undertaken to simulate dynamo processes within the earth and the convection zone of the sun. In these studies plausible models were used for both the α and ω effects. Some of the arbitrariness for the solar field was reduced in a study of Belvedere, Paterno and Stix (1980) in which the α -effect was modelled while the non-uniform rotation was calculated independently by Belvedere and Paterno (1977) on the assumption that latitude dependent heat transport sets up a meridional circulation which in turn causes the non-uniform rotation. In all of the studies mentioned above meridional circulation has been introduced and it has been shown that the inclusion of this circulation can greatly affect the critical parameters in the models. Roberts (1972) showed that for a particular model of the α and ω effects the presence of meridional flow can transform oscillatory dynamos into steady dynamos.

Another intriguing aspect of the previous studies is that in the case of axisymmetric systems steady solutions are associated with small values of the dynamo number, N , while for larger values of N the field is oscillatory.

In this article we consider axisymmetric dynamos of $\alpha^2\omega$ type when meridional circulation is present. The effect of meridional motion may play a crucial role in the solar dynamo since Schmidt (1982) has shown that for certain models of the convection zone the circulation speeds can be quite substantial with the θ component of

the velocity in the range 1–10 m/s at the solar surface and taking on larger values deeper down. Here we investigate the effects such large speeds will have on $\alpha^2\omega$ -dynamoes confined to an outer convection zone. We have included the α -effect generation of toroidal field from the poloidal field since one obtains modified critical behaviour to the purely $\alpha\omega$ situation. For dynamo action in general one question to consider is how do the large scale motions contribute towards the production of a dynamo given that the presence of turbulent motion is always necessary. We show that $\alpha^2\omega$ -dynamoes, and consequently $\alpha\omega$ -dynamoes, are associated with larger values for N because the presence of a small ω -effect is inhibitory to dynamo action. Furthermore since all estimates of α and ω for the sun yield a magnetic Reynolds number for the differential rotation greatly in excess of the α magnetic Reynolds number then it is usual to neglect the α -effect in producing the toroidal field. This neglect is computationally convenient since the equations may be scaled so that only one dynamo number is present. The relative influence of the α and ω effects is lost. However as we show below when meridional flow is present small changes in the magnitude of α can lead to qualitatively different dynamo action.

2. BASIC EQUATIONS AND METHOD OF SOLUTION

We consider a sphere of radius R and assuming symmetry about the rotation axis the mean field dynamo equations may be written as

$$\partial \mathbf{A} / \partial t = R_p (\mathbf{V}_p \times \nabla \times \mathbf{A}) + R_\alpha \alpha \mathbf{B}_T - \nabla \times (\nabla \times \mathbf{A}), \quad (1)$$

$$\begin{aligned} \partial \mathbf{B}_T / \partial t = & R_p \nabla \times (\mathbf{V}_p \times \mathbf{B}_T) + R_\omega \nabla \times [\mathbf{V}_T \times (\nabla \times \mathbf{A})] \\ & + R_\alpha \nabla \times \alpha (\nabla \times \mathbf{A}) - \nabla \times (\nabla \times \mathbf{B}_T), \end{aligned} \quad (2)$$

where the velocity and magnetic fields are respectively, $\mathbf{V} = \mathbf{V}_p + \mathbf{V}_T$ and $\mathbf{B} = \mathbf{B}_p + \mathbf{B}_T$ with $\mathbf{B}_p = \nabla \times \mathbf{A}$. All quantities are in dimensionless form and the magnetic Reynolds numbers R_α , R_ω and R_p are respectively $\alpha_0 R / \eta$, $\omega' R^3 / \eta$ and VR / η with the turbulent magnetic diffusivity, η , taken to be constant. Lengths are scaled by R and times are measured in terms of the diffusion time, R^2 / η . The

parameter α_0 is a measure of the α -effect while ω' is a measure of the gradient for the differential rotation. R_p parameterizes the mean meridional flow and V is taken to be a typical flow speed in the θ direction. We identify the dynamo number N as $R_\alpha R_\omega$. For pure $\alpha\omega$ -dynamoes the α term in equation (2) is neglected and $\mathbf{V}_p = \mathbf{0}$. For this case equations (1) and (2) may be rescaled (Roberts, 1972) so that only one parameter, $N^{1/2}$, appears in the equations. To consider $\alpha^2\omega$ -dynamoes with $\mathbf{V}_p \neq \mathbf{0}$ we find that in the numerical study of this problem it is convenient to rescale (1) and (2) by replacing \mathbf{A} by $R_\alpha \mathbf{A}$ so that the parameters appearing are R_α , N and R_p .

Following standard techniques (e.g. Krause and Rädler, 1980) originally due to Bullard and Gellman (1954), we expand the poloidal and toroidal parts of the magnetic field in the form

$$\mathbf{A}(x, \theta, t) = \left\{ 0, 0, e^{pt} \sum_{n=1}^M a_n(x) P_n^1(\cos \theta) \right\}, \quad (3a)$$

$$\mathbf{B}_T(x, \theta, t) = \left\{ 0, 0, e^{pt} \sum_{n=1}^M b_n(x) P_n^1(\cos \theta) \right\}, \quad (3b)$$

with $x = r/R$.

In the following we take, for simplicity,

$$\alpha = \alpha(x) \cos \theta \quad (4)$$

and $\alpha(x)$ is a function to be prescribed. Further, we suppose that the meridional circulation \mathbf{V}_p is solenoidal so that we may write

$$\mathbf{V}_p = \{v_r(x)P_2, v_\theta(x)P_2^1, 0\} \quad (5)$$

$$= \{2x^{-1}f(x)P_2, \frac{1}{3}x^{-1}[d(xf)/dx]P_2^1, 0\}, \quad (6)$$

and the exact form of f is discussed below. The toroidal velocity field is written as

$$\mathbf{V}_T = \{0, 0, x \sin \theta [1 + \omega_1(x) + \omega_2(x)P_2]\}, \quad (7)$$

where the form of ω_1 and ω_2 will depend on the model adopted.

Adopting the separation of variables as indicated by equations

(3)–(7) we eliminate the θ dependence by multiplying both sides of equations (1) and (2) by P_n^1 and integrating with respect to $\cos\theta$ between -1 and 1 . The resulting equations may be written as

$$\begin{aligned}
 pa_k &= a_k'' + 2x^{-1}a_k' - k(k+1)x^{-2}a_k + R_\alpha(c_1b_{k+1} + c_2b_{k-1}) \\
 &\quad - x^{-1}R_p v_r [c_3(xa_{k-2})' + c_4(xa_k)' + c_5(xa_{k+2})'] \\
 &\quad - x^{-1}R_p v_\theta (c_6a_{k-2} + c_7a_k + c_8a_{k+2}), \tag{8}
 \end{aligned}$$

$$\begin{aligned}
 pb_k &= b_k'' + 2x^{-1}b_k' - k(k+1)x^{-2}b_k - R_\alpha\{c_1[\alpha(xa_{k+1})]' \\
 &\quad + c_2[\alpha(xa_{k-1})]'\} + R_\alpha(c_{11}a_{k+1} + c_{12}a_{k-1}) \\
 &\quad - x^{-1}R_p [c_3(xv_r b_{k-2})' + c_4(xv_r b_k)' + c_5(xv_r b_{k+2})'] \\
 &\quad + x^{-1}R_p v_\theta (c_{10}b_{k-2} + c_7b_k + c_9b_{k+2}) \\
 &\quad + R_\omega\{\omega_1'(c_{13}a_{k-1} + c_{14}a_{k+1}) + \omega_2'(c_{15}a_{k-3}) + c_{16}a_{k-1} \\
 &\quad + c_{17}a_{k+1} + c_{18}a_{k+3}\} - x^{-1}\omega_2 [c_{19}(xa_{k-3})' + c_{20}(xa_{k-1})' \\
 &\quad + c_{21}(xa_{k+1})' + c_{22}(xa_{k+3})']\}; \tag{9}
 \end{aligned}$$

where dashes are differentiation with respect to x and the $c_i = c_i(k)$ where $k = 1, 2, \dots, M$. The c_i are listed in the Appendix.

The coupled equations (8) and (9) divide naturally into two families: (i) the dipolar type (a_{2k-1}, b_{2k}) with the field anti-symmetric with respect to the equator and (ii) the quadrupolar type, (a_{2k}, b_{2k-1}) which are symmetric with respect to the equator. These equations are to be solved subject to the boundary conditions.

i) For a sphere,

$$a_k(0) = b_k(0) = 0 \tag{10}$$

and

$$a_k'(1) + (k+1)a_k(1) = b_k(1) = 0. \tag{11}$$

ii) For a shell with an inner radius of $x=x_u$ the boundary conditions (10) is replaced by

$$a_k(x_u) = (xb_k)'_{x=x_u} = 0. \quad (12)$$

This condition was used by Belvedere, Paterno and Stix (1980) and is a special case of general boundary condition given by Roberts (1972). The use of this boundary condition presupposes that a field within the shell (convection zone) is unable to penetrate into the (radiative) core which has a much higher conductivity. When dynamo action is present equation (12) is strictly only valid when the α -effect vanishes on x_u and the dynamo field is oscillatory. In his numerical studies on shells Roberts (1972) took both a_k and b_k to be zero on x_u and conjectured that the error would be small. In our calculations we found that using the different conditions leads to differences in the critical numbers of the order of 4 percent or less for the oscillatory modes. To determine the eigenvalue, p , in equations (8) and (9), the derivatives are replaced by finite differences and the system is solved as an algebraic eigenvalue problem

$$A\mathbf{x} = p\mathbf{x},$$

with the dimension of A determined by M , the truncation level for the field expansions and m the number of grid points. For most of the results reported here M was taken to be 5 and 6 while m ranged from 20 to 40. The convergence of solutions for larger values of M is well established. Furthermore the results for $\alpha\omega$ -dynamos are stable to variations in m . Since we were interested in establishing general trends for arbitrary models it did not seem worthwhile in terms of computing time to pursue the precise details of the convergence properties of the critical numbers. As a check on our numerical procedures we compared our solutions with previous authors. In all cases the agreement was satisfying as will be indicated below.

Since we shall be looking at the growth rates of the eigenvalues with R_m , the appropriate magnetic Reynolds number, it is pertinent to recall that for a sphere the free decay modes in the absence of fluid motion may be found analytically (Moffatt, 1978). The slowest decaying mode is $p = -\pi^2$ for the dipolar fields while the quadrupolar fields have $p = 20.19$.

For a shell with the boundary conditions given by (12) the poloidal decay modes are given by the roots of

$$J_{k+1/2}(Kx_u) J_{1/2-k}(K) - J_{-(k+1/2)}(Kx_u) J_{k-1/2}(K) = 0,$$

where $K = -p^2$. For $k=1$ this expression reduces to the non-trivial roots of $\tan K(x_u - 1) = Kx_u$. When $x_u = 0.7$ then $p \sim -36.2$. This large value of $|p|$ for a field confined to a shell implies that larger Reynolds numbers will be needed to excite the field to its critical state than for the case of a field in a sphere.

3. MODELS FOR A SPHERE

For the situations where dynamo action is possible throughout a sphere we considered two models which have appeared in the literature (Steenbeck and Krause, 1966; Roberts, 1972 and Jepps, 1975).

Model 1

$$\alpha = 1, \quad \omega_1 = -x, \quad f = 7168(2)^{1/2}x^6(1-x)^2/243.$$

Model 2

$$\alpha = 729x^8(1-x^2)^2/16, \quad \omega_1 = 19683(1-x^2)^5/40960, \quad \text{and } f \text{ as for } \textit{Model 1}.$$

In both models the α -effect is positive in the northern hemisphere while ω_1 is negative. Model 1 is probably quite artificial, however it does provide a model in which the α and ω effects are uniform throughout the sphere. In Model 2 the maxima for the two induction effects are separated. Stix (1973) concludes that the oscillating nature of $\alpha\omega$ -dynamos is due to the geometry of the induction effects. Since these two models have different geometries we conclude below that the oscillatory nature of $\alpha\omega$ -dynamos is due to the driving mechanism of the ω -effects.

For α^2 -dynamos with $R_\omega = R_p = 0$ the field is maintained by the turbulent motions alone. For Models 1 and 2 the critical values of R_α (with $M=6$ and $m=40$) are shown in Table I with the values

TABLE I

Model	Dipole	Quadrupole
1	7.66 (7.64)	7.85 (7.80)
2	13.08 (13.04)	13.43 (13.11)

obtained by Roberts (1972) in parentheses. For larger values of R_α the values of $\text{Re } p$ increase steadily away from zero with higher modes also having $\text{Re } p > 0$, e.g. Model 1 with $R_\alpha = 12$ gives $\text{Re } p = 18.52$ and 1.22 (dipolar); and $\text{Re } p = 18.54$ and 1.43 (quadrupolar). Holding $R_\omega = 0$ we introduced a meridional circulation in both models. When R_α was at its critical value then for $|R_p| \neq 0$ the dynamo fails while for R_α values above critical the values of $\text{Re } p$ monotonically decrease with increasing $|R_p|$. To excite α^2 -dynamos in the presence of circulation requires larger values of R_α than in the zero circulation situation. The inhibiting effect of circulation on α^2 -dynamos (with dipolar parity) was also found by Hellmich (1978) in a dynamical calculation. Our result differs in some respects to Rädler (1975) where a different model was used. In terms of the parameter used here Rädler finds that for the dipolar field the dynamo is inhibited for $-6 < R_p < 3$. Values of R_p outside this range lead to an enhancement of dynamo action. For the quadrupolar mode the dynamo is inhibited only when $0 < R_p < 8$. In view of the comments below, results for large values of $|R_p|$ need to be treated with some caution.

For the meridional circulation model studied here the flow consists of simple closed streamlines. From the work of Weiss (1966) we know that the poloidal flux will be expelled from the region of flow. The timescale of flux expulsion will be of the order $t_{fe} = R_p^{1/3} t_c$ (Moffatt and Kamkar, 1982) where t_c is the turnover time. In terms of the diffusion time, t_D , $t_c = t_D/R_p$ and so $t_{fe} = t_D R_p^{-2/3}$. For large values of R_p the flux is expelled well within the diffusion time. The eigenvalue method used here will not be reliable for R_p too large (for fixed α) since \mathbf{B}_p will be negligible and the numerical results will be unstable. We indeed found this to be so when the pure diffusion case was examined for large values of R_p (for sphere $R_p > 30$). Increasing R_p is the absence of any dynamo action requires finer and finer grids to be used to obtain reliable spatial resolution. It is the rate of the

poloidal flux expulsion which determines the values of R_p which may be used.

We now consider the ω -effect by putting $R_p=0$ and allow R_ω to increase away from zero. As Roberts and Stix (1972) have shown for a particular α and ω model due to Steenbeck and Krause (1969) for $\alpha^2\omega$ -dynamos there is a transition region for the ratio R_α/R_ω over which the dynamo changes from being steady to being oscillatory. Both R_α and R_ω take their critical values over the range they studied. For $R_\alpha/R_\omega < 10^{-3}$ they found that the dynamo is purely $\alpha\omega$ while for $R_\alpha/R_\omega > 10^{-1}$ the dynamo is stationary and they concluded that the α^2 -effect was dominant. Obviously for values between these two extremes the α -effect will assist in the production of toroidal field to a great or lesser extent. It is well established that oscillatory $\alpha\omega$ -dynamos are associated with large values of $N^{1/2}$ while the steady α^2 -dynamos are associated with modest values of magnetic Reynolds numbers. To see why this should be so we held R_α constant at the critical values for the two models and increased R_ω . The effect on $\text{Re } p$ is shown schematically in Figures 1 and 2 for the dipolar and quadrupolar modes respectively. For Figures 1 and 2 the horizontal axis, R_m , represents the relevant magnetic Reynolds number, i.e. either R_α or R_ω , each one varying as indicated in the diagrams. As can be seen from the sketches the behaviour of $\text{Re } p$

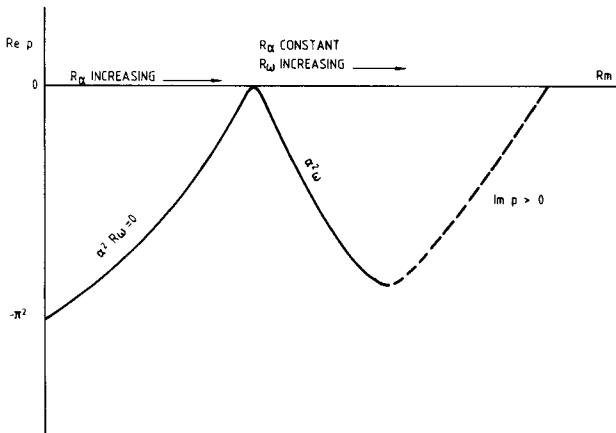


FIGURE 1 A schematic plot of the growth rate of $\text{Re } p$ for the dipolar fields of Models 1 and 2. R_α is increased to obtain a critical R_m , then holding R_α constant R_ω is increased until R_m is again critical. The solid line corresponds to $\text{Im } p = 0$.

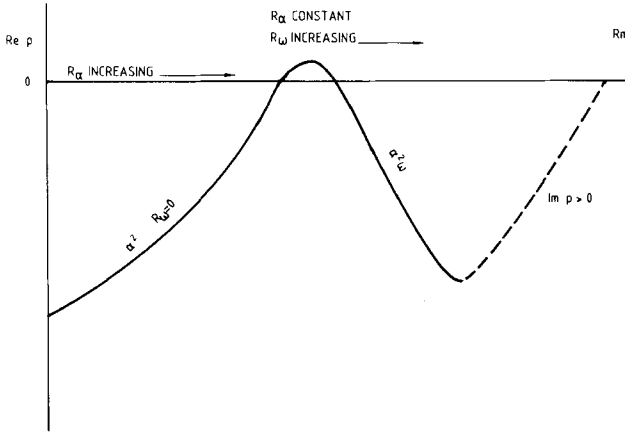


FIGURE 2 The same as for Figure 1 with dipolar replaced by quadrupolar.

with R_m for the dipolar and quadrupolar parities is different above the critical value for R_α . However the fact the $\alpha^2\omega$ and consequently $\alpha\omega$ -dynamoes are associated with large values of R_m is clearly illustrated. The ω -effect is inhibitory to dynamo action for small values of R_ω for fields of dipolar parity provided $\partial\omega_1/\partial x < 0$.

In Figure 2 it can be seen that the quadrupolar fields are enhanced for a weak rotational shear [e.g. see Rädler (1975)] however when the relative importance of the α^2 -effect is decreased again large values of N are required to restore the dynamo. Furthermore there is a critical value for R_ω at which the eigenvalue associated with the (decaying) field changes from being real to being complex. For values of R_ω above this value the steady increase of $\text{Re } p$ is associated with a non-zero $\text{Im } p$. The fact that $\text{Re } p$ does increase is due to the transition from real to complex p as was found for a number of $\alpha\omega$ -dynamoes discussed by Deinzer *et al.* (1974). The product $R_\alpha R_\omega$ then reaches a critical value when dynamo action is again present. The critical values of R_ω are given in Table II and the oscillation frequencies are given in parentheses. The ratio R_α/R_ω for Model 1 is ~ 0.02 , while for Model 2 the ratio is ~ 0.08 for both parities. Establishing an $\alpha^2\omega$ -dynamo by this procedure leads to the preferred mode being model dependent. The results for Model 1 are consistent with the findings of Roberts (1972) for an $\alpha\omega$ -dynamo whereas the results for Model 2 indicate that the preferred mode is

TABLE II
Values of R_ω and $\text{Im } p$.

Model	Dipole	Quadrupole
1	349.0 (28.6)	522.3 (27.4)
2	1705.2 (27.96)	1598.6 (17.6)

quadrupolar. It should be stressed however that these values of R_α and R_ω are not necessarily optimal in establishing a dynamo. However what we have shown is that the size of the α -effect relative to the ω -effect must be crucial in determining the preferred mode. The field lines for the α^2 and $\alpha^2\omega$ -dynamos for Model 2 are shown in Figures 3–6.

Having established an $\alpha^2\omega$ -dynamo we again introduced meridional circulation. The results here are qualitatively different from those for the α^2 -dynamo. The results are model dependent in that for Model 1, $R_p=2$ causes the dynamo to fail for both dipolar and quadrupolar parities, while for $R_p=-2$ the dynamo is enhanced. For Model 2 the situation is reversed in that $R_p>0$ leads to an enhancement of the dynamo action with a decrease in the oscillation frequency of the field. For $R_p=20$ we find $R_\omega=1315.2$, $\text{Im } p=7.8$ for the dipolar field and $R_\omega=722.3$ ($\text{Im } p=0$) for the quadrupolar mode with R_α held at the critical values found previously. For the single cell circulation used here we find that the quadrupole mode is more easily excited and this was found to be the case in the shell calculations reported in the next section. Assuming that the circulation is in the direction of from poles to equator ($R_p>0$), which would be consistent with an $\omega(r,\theta)$ increasing inward, [e.g. see Kohler (1974)] then the enhancement of dynamo action could be due to a tendency for the flow to push the flux into the region of maximum toroidal shearing. For Model 2 this maximum is at $x=0.33$. In Model 1 the shearing is uniform throughout the sphere.

Roberts (1972) found that for R_p sufficiently large then the preferred solutions were always steady in the case of $\alpha\omega$ -dynamos. For Model 2 we looked at the quadrupole mode and for $R_p=-20$ with R_ω constant we increased the value of R_α and for $R_\alpha=15.4$ we

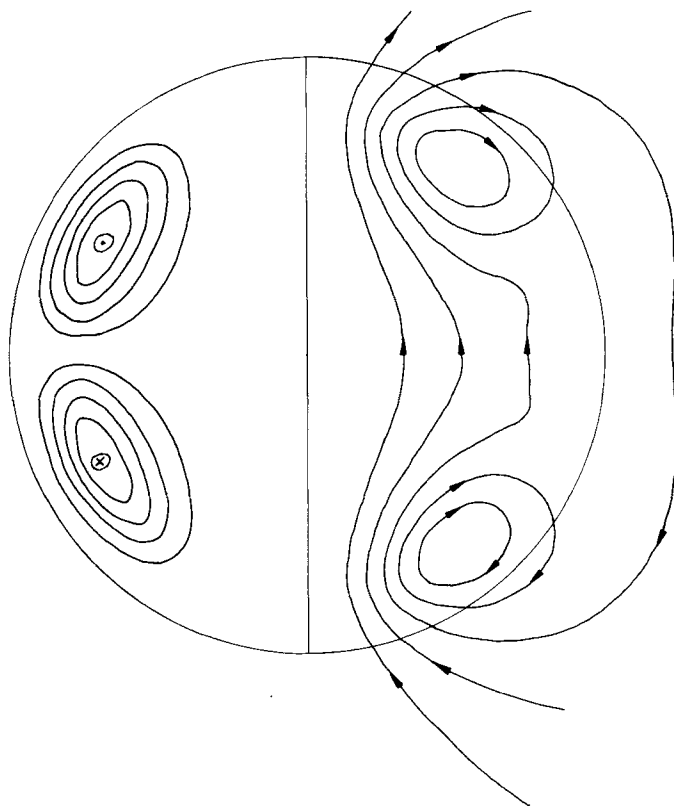


FIGURE 3 Dipolar α^2 dynamo for Model 2. The B_P lines are shown on the right and lines for $B_T = \text{constant}$ are on the left. An encircled dot (cross) indicates a vector pointing out (into) the plane of the paper. The contours mark the levels $\pm\frac{1}{6}, \dots, \pm\frac{2}{3}$ times the maximum values of the toroidal and poloidal fields.

found that the dynamo could be restored and in this case it was steady.

4. MODELS FOR A SHELL

We now consider dynamo action which is confined to a shell of radius $x = x_u = 0.7$. As a model of the solar convection zone we envisage that fields which are produced in the turbulent layer do not

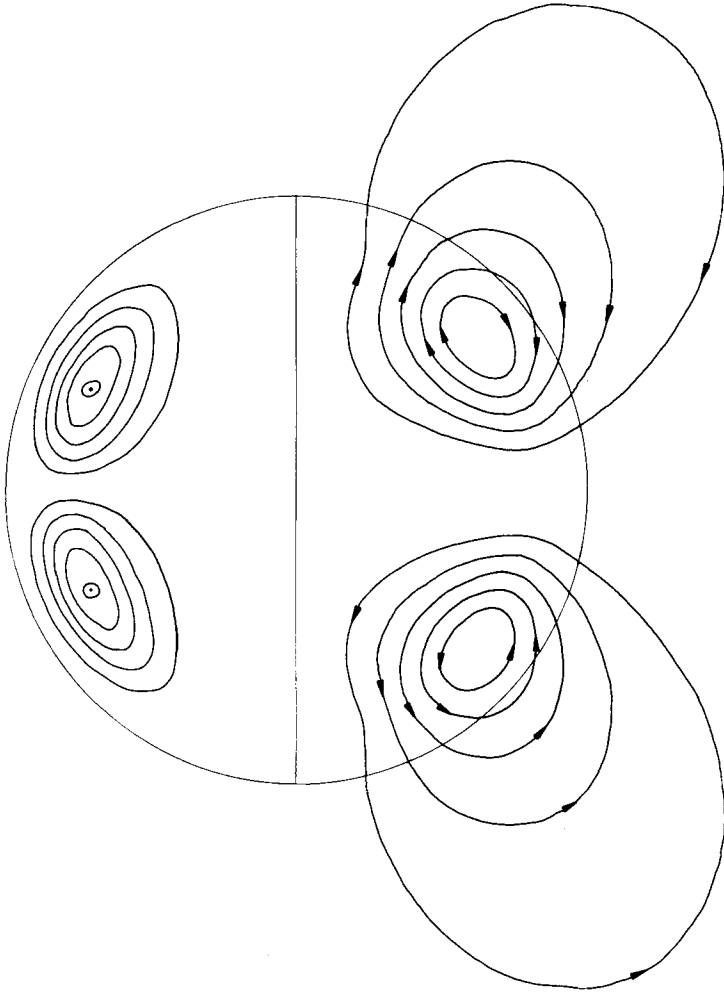


FIGURE 4. Quadrupolar α^2 dynamo for Model 2. Otherwise as for Figure 3.

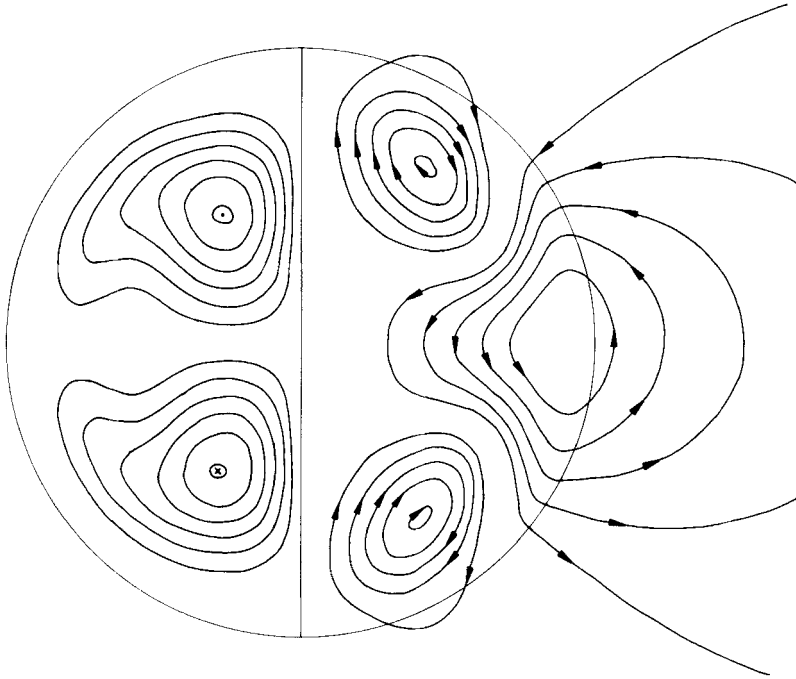


FIGURE 5 Dipolar $\alpha^2\omega$ dynamo for Model 2 with $t=0$. Otherwise as for Figure 3.

penetrate into the radiative core and the boundary conditions given by equation (12) apply.

We considered the following models:

Model 3

$$\alpha=1, \quad \omega_1=1-x,$$

$$\psi_p = [4(x-x_u)(1-x)/(1-x_u)^2]^3 \sin^2\theta \cos\theta \equiv f \sin^2\theta \cos\theta,$$

where ψ_p is the stream function for the meridional flow (Roberts and Stix, 1972; Krause and Rädler, 1980). The streamlines are shown in Figure 7.

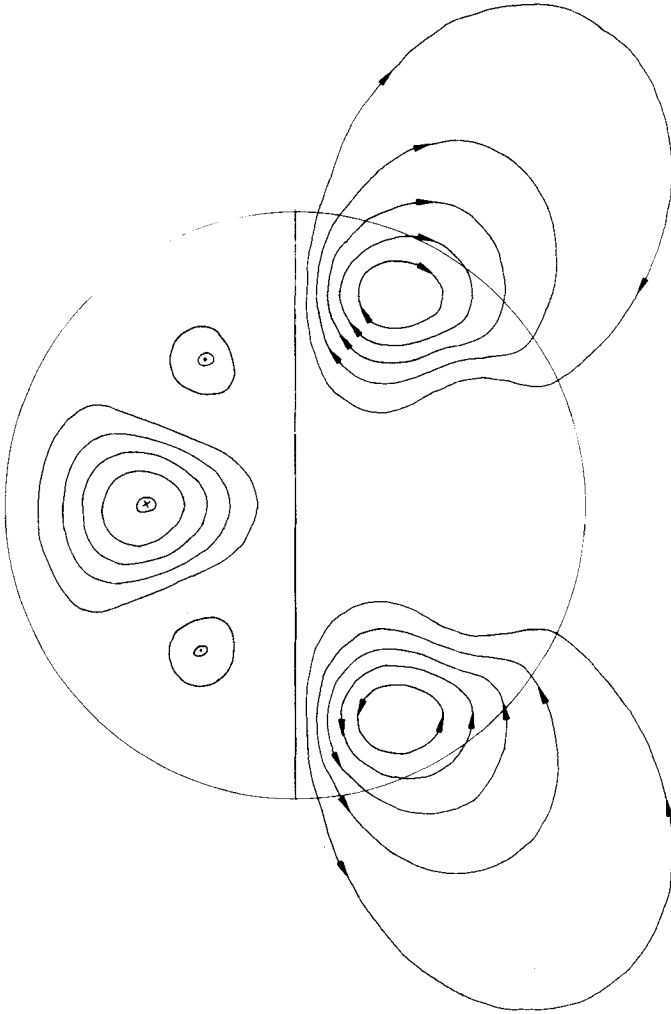


FIGURE 6 Quadrupolar $\alpha^2\omega$ dynamo for Model 2 with $t=0$. Otherwise as for Figure 3.

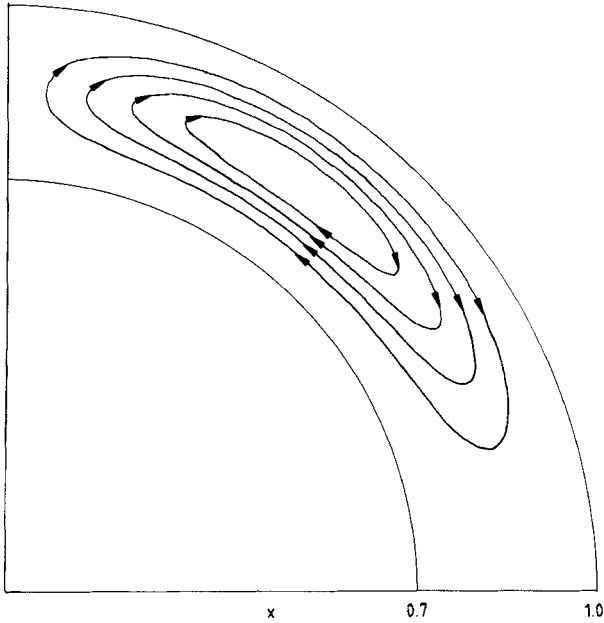


FIGURE 7 Streamlines for a single cell meridional velocity field. The flow is restricted to the region $0.7 < x < 1$. The direction of the flow is for $R_p > 0$.

Model 4

As for Model 3 with

$$\omega_1 = \frac{1}{2} \{ 1 - \text{Erf} [(x - x_u)/0.075] \}.$$

Model 5

As for Model 4 with ω_1 centred at $x=0.8$.

Model 6

$$\alpha = 27(1-x)(x-x_u)^2/4(1-x_u)^3,$$

ω_1 and ψ_p as for Model 4.

In Model 6 the variation of α with x is the model used by Belvedere, Paterno and Stix (1980) where α is small at both the top and bottom of the convection zone. Cowling (1981) has pointed out that the α -effect should be present throughout the convection zone so in the absence of any detailed knowledge of α , allowing α to act over the whole shell is a plausible assumption. The models studied here have this property. The form of ω_1 used in Models 4-6 is consistent with one of the models of Schmidt (1982) where the differential rotation is independent of θ and steadily decreases from the inner boundary of the shell. In Models 4 and 6 the influence of the shear is confined to a small region near the lower boundary. It has been conjectured by Schüssler (1982) that dynamo fields are concentrated in the "overshoot layer" of the convection zone which operates at the interface of the convective and radiative zones. The magnitude of the toroidal field is far greater than the poloidal component and Models 4-6 place the production of the toroidal field in this "overshoot layer".

The critical numbers for the models when treated as $\alpha\omega$ -dynamos are given in Table III. The differences between Models 4 and 6 are due to the variation in α with x . For fixed R_ω the increase in the critical number is then due to an increased R_α value and this conclusion is in agreement with the findings of Belvedere, Paterno and Stix (1980) for a particular model for the ω -effect.

TABLE III
Critical values for the dipolar modes

Model	N	$\text{Im } p$
3	1.7×10^4	76.8
4	3.6×10^4	105.3
5	8.4×10^3	142.5
6	8.2×10^4	137.0

The differences between Models 4 and 5 is due to the location of the maximum in the toroidal shearing where in Model 5 this maximum is away from the boundary and this leads to an increase in the oscillation of the field.

For Model 6 we considered it in the context of an $\alpha^2\omega$ -dynamo and varied R_α . For $R_\alpha=8$ the critical dynamo number for the dipolar

mode was 7.5×10^4 with $\text{Im } p = 131.7$ while for $R_\alpha = 18$, $N = 6.3 \times 10^4$ with $\text{Im } p = 107.0$. The increase in α is again associated with a decrease in the frequency of the field.

For the $\alpha\omega$ -dynamo using Model 5 we introduced meridional circulation. There is no agreement as to the speed of the meridional flow in the convective zone however we may use some results found by Schmidt (1982). In the models computed by Schmidt the solar differential rotation is driven by either latitude dependent heat transport or anisotropic viscosity. The results for both mechanisms depend crucially on the boundary conditions and the value chosen for the Prandtl number. Schmidt obtains speeds at the surface which may then vary from $v_\theta \ll 1 \text{ ms}^{-1}$ to $V_\theta \geq 10 \text{ ms}^{-1}$. For $V_\theta \lesssim 1 \text{ ms}^{-1}$ the number R_p in our calculations may vary from $\lesssim 10$ to ~ 35 depending on the magnitude of η .

As an estimate of η we have assumed the values $(2-5) \times 10^7 \text{ m}^2 \text{ s}^{-1}$. Belvedere and Paterno (1977) have also performed similar calculations for meridional flows driven by latitude dependent heat transport. In their models the circulation speeds were $\ll 1 \text{ ms}^{-1}$ at the solar surface and the circulation consisted of a single cell. In the models calculated by Schmidt the circulation was not confined to a single cell. To account for this albeit in an *ad hoc* way we introduced a stream function given by

$$\psi_p = [64(x - x_u)^3(1 - x)^3(x_b - x)/(1 - x_u)^6] \sin^2 \theta \cos \theta \equiv f \sin^2 \theta \cos \theta.$$

The streamlines for the flow when $x_b = 0.86$ are shown in Figure 8.

For Model 5 as an $\alpha\omega$ -dynamo Figure 9 shows the field pattern without circulation. The introduction of a double cell circulation with $R_p = 35$ does not noticeably alter the field pattern and we found that $N^{1/2} = 88.5$ while $\text{Im } p = 145.9$. For larger values of R_p the dynamo is excited for smaller values of $N^{1/2}$ and the frequency does not vary a great deal. For this model the circulation assists in the production of a dynamo in the sense that the dynamo is more easily excited in terms of smaller values of $N^{1/2}$. Model 5 produces a field with different structure in the case of the single cell circulation. For $R_p > 0$ dynamo action is inhibited and consequently larger values of $N^{1/2}$ are needed to excite the dynamo. In Figure 10 we show the case for $R_p = 10$ and the critical numbers are now $N^{1/2} = 111.8$ with $\text{Im } p = 169.6$. For this situation the poloidal field lines follow the fluid

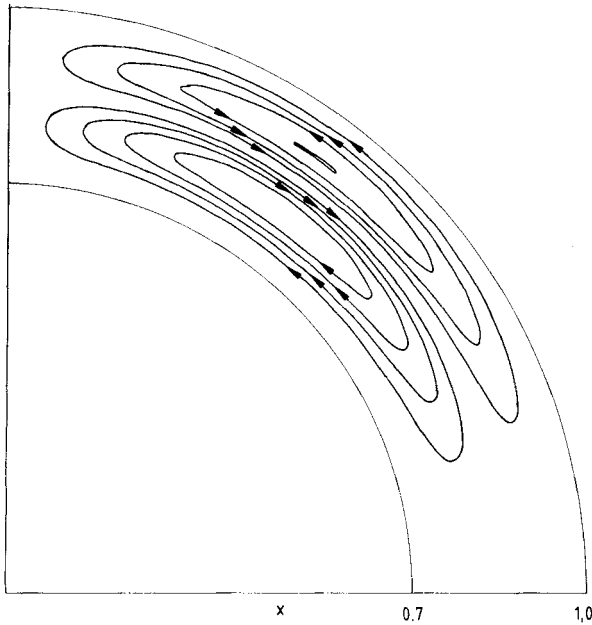


FIGURE 8 Streamlines for a double cell meridional velocity field. The direction of the flow is for $R_p > 0$.

lines as the field now has to act against the fluid flow which being a single cell type has a tendency to expel the field. Noticeably the field is concentrated beneath the surface. In Figure 11 we have the field lines for a supercritical field in the presence of double cell circulation where $N^{1/2} = 91.5$, $R_p = 100$, $\text{Re } p = 10.4$ and $\text{Im } p = 169.7$. The field has moved towards the poles while the field lines have been pulled beneath the surface.

In Model 5 the position of maximum toroidal shearing is located away from the boundary and we find that we have somewhat different results when we consider Model 6 where the toroidal shearing is confined to a region near the lower boundary of the shell. For Model 6 as an $\alpha^2\omega$ -dynamo with $R_\alpha = 8$ we find that the presence of a single cell circulation with $R_p < 3$ enhances dynamo action while lowering the value of $\text{Im } p$. This is true for both dipolar and quadrupolar parities. As R_p is steadily increased then the circulation destroys the dynamo and larger and larger values of N

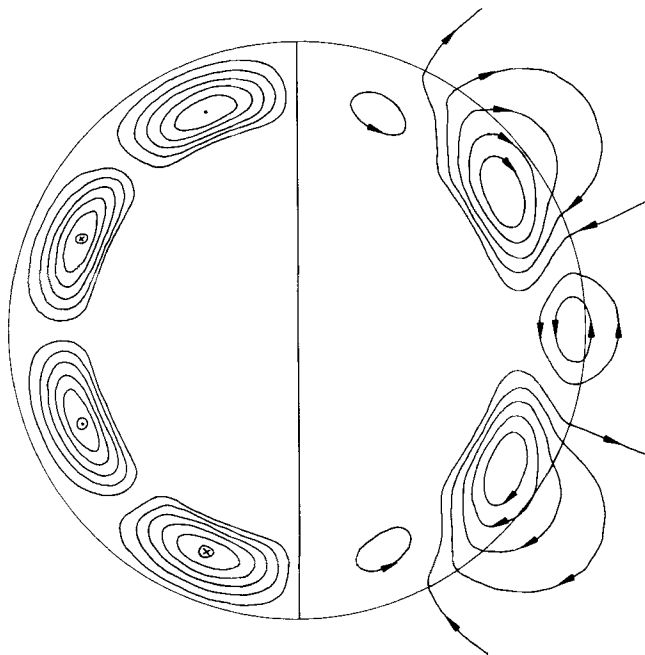


FIGURE 9 Dipolar $\alpha\omega$ dynamo for Model 5. (i) $N^{1/2} = 91.5$, $R_p = 0$ and (ii) $N^{1/2} = 88.5$, $R_p = 35$ (2 cell); at the instant $t = 0$. Otherwise as for Figure 3.

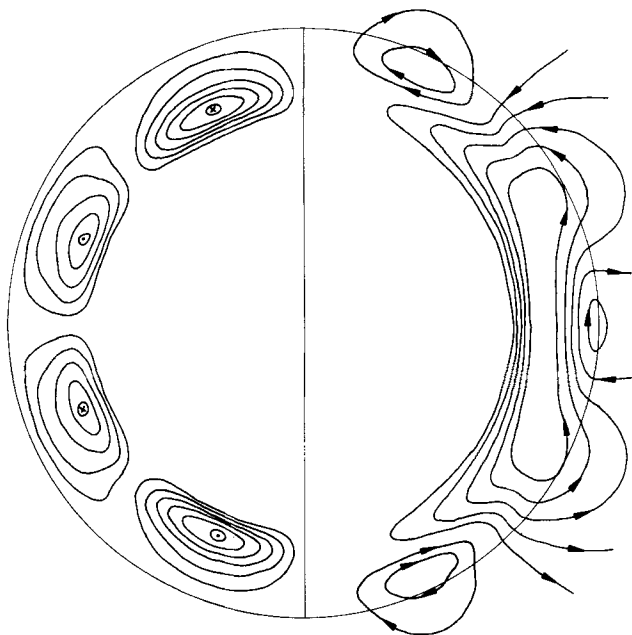


FIGURE 10 Dipolar $\alpha\omega$ dynamo for Model 5 $N^{1/2} = 111.8$, $R_p = 10$ (1 cell), and $t = 0$. Otherwise as for Figure 3.

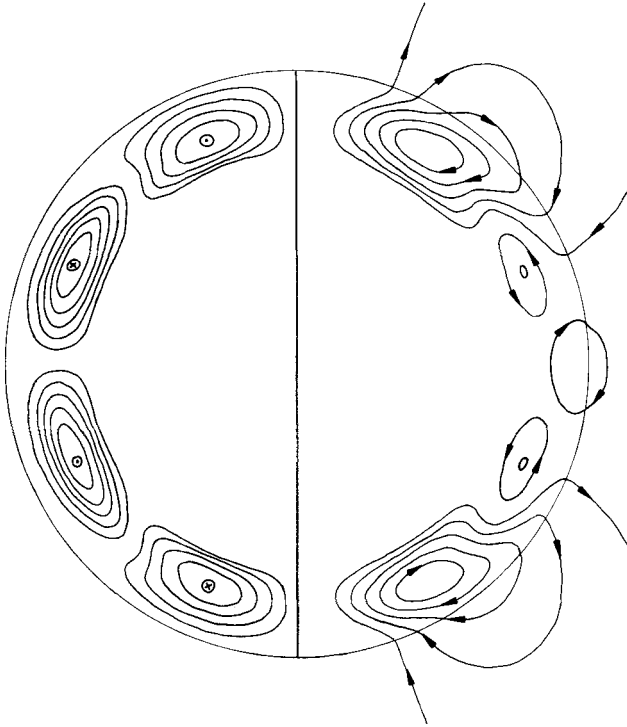


FIGURE 11 Supercritical $\alpha\omega$ dynamo for Model 5. $N^{1/2}=91.5$, $R_p=100$ (2 cell) $\text{Re } p=10.42$, $\text{Im } p=169.7$, and $t=0$. Otherwise as for Figure 3.

are needed to restore the field to its critical state. When circulation is present the quadrupolar mode is the one which is marginally easier to excite. For $R_p=10$ the critical numbers are 11.9×10^4 ($\text{Im } p=124.5$) and 12.4×10^4 ($\text{Im } p=128.7$) for the quadrupolar and the dipolar parities respectively.

The quadrupolar field for $R_\alpha=8$ has 12.2×10^4 and $\text{Im } p=142.1$ when the circulation is absent. For $R_p < 0$ the dynamo fails for both parities though as was found by Roberts and Stix (1972) the dipole field is the one most readily restored. For the simple model of the circulation we have used it would be necessary to have the surface flow moving from equator to pole in order to ensure that the dipolar field was dominant. In Figure 12 we show the dipolar field for

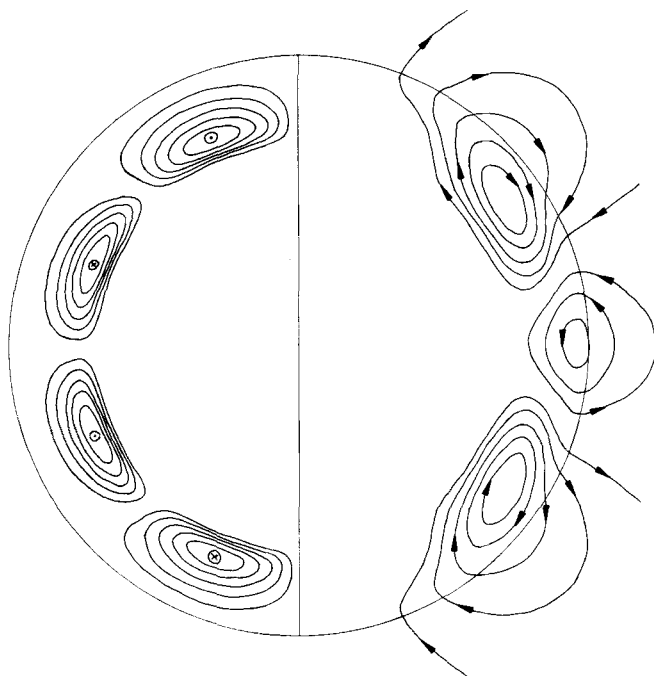


FIGURE 12 Dipolar $\alpha^2\omega$ dynamo for Model 6 for (i) $R_\alpha=8$, $R_\omega^{1/2}=98.85$, $R_p=0$, (ii) $R_\alpha=8$, $R_\omega^{1/2}=124.5$, $R_p=10$ (1 cell); and $t=0$. Otherwise as for Figure 3.

Model 6 with $R_\alpha=8$ and $R_\omega^{1/2}=98.85$ in the absence of circulation. After introducing a single cell circulation and setting $R_p=10$ we obtain an almost identical field pattern if the dynamo is restored by varying R_ω . The relevant numbers are now $R_\alpha=8$, $R_p=10$ and $R_\omega^{1/2}=124.5$. This result is reasonable since for the single cell circulation models of Belvedere and Paterno (1977) the meridional circulation drives the differential rotation and consequently a relative increase in the ω -effect is going to offset the inhibitory effect of the circulation.

Holding $R_\omega^{1/2}=98.85$ and allowing R_α to increase we obtain the field pattern shown in Figure 13. The critical value for R_α is now 12.0. The poloidal field lines now have a tendency to follow the streamlines of the circulation. Consistent with the findings for dynamos in a sphere the increase in the α -effect is accompanied by a decrease in $\text{Im } p (=122.8)$.

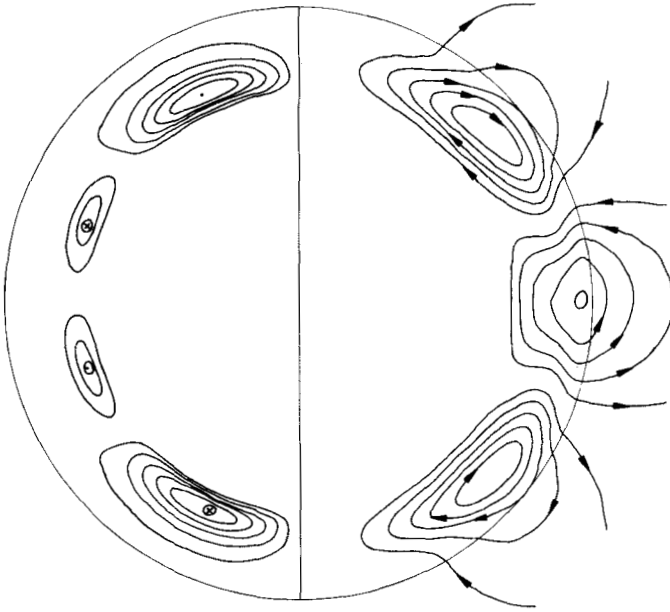


FIGURE 13 Dipolar $\alpha^2\omega$ dynamo for Model 6 for $R_\alpha=12$, $R_\omega^{1/2}=98.85$ and $R_p=10$ (1 cell), and $t=0$. Otherwise as for Figure 3.

When the double cell circulation is present the dipolar mode is the one more readily excited for $R_p > 0$. For the circulation considered here this means that the flow at the surface is towards the poles. The presence of the circulation leads to higher values for the frequency of the field as was found for Model 5. If the direction of the flow is reversed then the quadrupolar mode is the one more easily excited. However all the models of Schmidt are equivalent to $R_p > 0$ and so based on the simple model considered here double cell flows would lead to dipolar fields being the dominant mode.

For the models we have computed it was noticed that the oscillation frequencies for fields confined to shells are a good deal larger than the frequency for Model 1 of Steenbeck and Krause (1969) where the field occupies the whole sphere. We computed the critical values for this model and obtained $N^{1/2} = 144.6$ ($\text{Im } p = 31.1$). When the field is confined to a shell we obtained $N^{1/2} = 412.6$ and $\text{Im } p = 77.7$ and the frequency of the field has increased.

For Models 4–6 and for this model also the period of the oscillatory field given by $2\pi R^2/\eta \text{Im } p$ lies in the range 15–45 years depending on the model and the value of η chosen.

For all of the models studied here we found that if R_p is increased beyond some limit then the critical eigenvalue is real and consequently the field is steady. This result occurred using the modified boundary conditions $a_k(x_u) = b_k(x_u) = 0$. The boundary conditions were then altered to account for $\text{Im } p = 0$, and the results were modified by less than 3%. For the single cell circulation the value of $R_p \sim 15$ yielded an $\text{Im } p = 0$. Larger values of R_p could be attained for the double cell flow before the field turned steady. We did not search for the critical R_p for each model though it appears that $R_p > 150$. For the single cell flow it may be argued that if the poloidal field is to be maintained against flux expulsion then it would be necessary to increase the relative weighting of the α -effect and, as we have shown, this leads to steady fields.

Finally we looked at Model 6 in the absence of circulation with the differential rotation now containing a term proportional to $P_2(\cos\theta)$. We adopted the model of Roberts and Stix (1972) in which the solar core rotates more rapidly than the convection zone. This model has the form

$$\omega_1 = \frac{2}{3}\beta + \frac{1}{2}(1 - \frac{2}{3}\beta)\{1 - \text{Erf}[(x - x_u)/0.075]\}$$

and

$$\omega_2 = -\frac{1}{3}\beta\{1 + \text{Erf}[(x - x_u)/0.075]\},$$

where β is a parameter which varies between 0 and 1. For $R_\alpha = 8$ the dynamo is critical when $R_\omega^{1/2} = 57.8$ and $\text{Im } p = 287.9$. The frequency of the field is larger than for the case when the differential rotation is a function of r only.

When the dynamo is critical then the introduction of double cell circulation leads to enhancement of dynamo action with a corresponding increase in $\text{Im } p$. For example when $R_p = 35$ with R_α and R_ω held at the values above then $\text{Re } p = 2.04$ and $\text{Im } p = 289.8$. Again this type of circulation is the one which assists in the production of a dynamo.

5. REMARKS

Using the simple models studied here we may conclude that for dynamo action in shells meridional flows with a double cell structure will assist in the production of an oscillatory dynamo of dipolar type. This result seems to be independent of the choice of location of the maximum in the toroidal shearing and whether the differential rotation is a function of r and θ or r only.

For single cell flows the dynamo is enhanced for small numbers of revolutions per diffusion time provided the toroidal shearing is located near the lower boundary of the convection zone. In this case the direction of flow will determine which mode is favoured. For increasing R_p , dynamo action is inhibited independent of the location of the maximum of ω' . For this situation the field is expelled from the central regions and the study of the resulting boundary layer problem would be necessary to analyse the behaviour of the dynamo action in this region.

References

- Belvedere, G. and Paterno, L., "Convection in a rotating deep compressible spherical shell—application to sun," *Sol. Phys.* **54**, 289 (1977).
- Belvedere, G., Paterno, L. and Stix, M., "Dynamo action of a mean flow caused by latitude-dependent heat-transport," *Astron. & Astrophys.* **86**, 40 (1980).
- Bullard, E. C. and Gellman, H., "Homogeneous dynamos and terrestrial magnetism," *Philos. Trans. R. Soc. London A* **247**, 213 (1954).
- Cowling, T. G., "The present status of dynamo theory," *Annu. Rev. Astron. & Astrophys.* **19**, 115 (1981).
- Deinzer, W., Kusserow, H.-U.v. & Stix, M., "Steady and oscillatory alpha-omega dynamos," *Astron. & Astrophys.* **36**, 69 (1974).
- Hellmich, R., "Finite amplitude α^2 -dynamos with large scale incompressible circulation," *Geophys. & Astrophys. Fluid Dyn.* **10**, 89 (1978).
- Jepps, S. A., "Numerical model of hydromagnetic models," *J. Fluid Mech.* **67**, 625 (1975).
- Köhler, H., "Differential rotation," *Sol. Phys.* **34**, 11 (1974).
- Krause, F. and Rädler, K. H., *Mean-field Magnetohydrodynamics and Dynamo Theory*, Pergamon, Oxford (1980).
- Moffatt, H. K., *Magnetic Field Generation in Electrically Conducting Fluids*, CUP (1978).
- Moffatt, H. K. and Kamkar, H. in Proceedings of the Workshop on *The Theory of Stellar and Planetary Magnetism*, Budapest (1982).

- Rädler, K. H., "Some new results on the generation of magnetic fields by dynamo action," *Mém. Soc. R. Sci. Liege 6^e serie VIII*, 109 (1975).
- Roberts, P. H., "Kinematic dynamo models," *Philos. Trans. R. Soc. London A* **272**, 663 (1972).
- Roberts, P. H. and Stix, M., "Alpha-effect dynamos, by Bullard-Gellman formalism," *Astron. & Astrophys.* **18**, 453 (1972).
- Schmidt, W., "Models of solar differential rotation," *Geophys. & Astrophys. Fluid Dyn.* **21**, 27 (1982).
- Schüssler, M. in "Solar and Stellar Magnetic Fields, Origins and Coronal Effects," *IAU Symp.* **102**, Zurich (1982).
- Steenbeck, M. and Krause, F., "Erklärung stellarer und planetarer Magnetfelder durch einen turbulenzbedingten Dynamomechanismus," *Z. Naturforsch.* **219**, 1285 (1966).
- Steenbeck, M. and Krause, F., "Zur Dynamotheorie stellarer und planetarer Magnetfelder I. Berechnung sonnenähnlicher Wechselfeldgeneratoren," *Astron. Nachr.* **291**, 49 (1969).
- Stix, M., "Spherical alpha-omega dynamos by a variational method," *Astron. & Astrophys.* **24**, 275 (1973).
- Weiss, N., "Expulsion of magnetic flux by eddies," *Proc. R. Soc. London Ser. A* **293**, 310 (1966).

Appendix

$$c_1 = \frac{k+2}{2k+3},$$

$$c_{12} = k^2 c_2,$$

$$c_2 = \frac{k-1}{2k-1},$$

$$c_{13} = k c_2,$$

$$c_3 = \frac{3(k-1)(k-2)}{2(2k-3)(2k-1)},$$

$$c_{14} = -(k+1)c_1,$$

$$c_4 = \frac{k^2+k-3}{(2k+3)(2k-1)},$$

$$c_{15} = \frac{3(k-3)(k-2)^2(k-1)}{2(2k-5)(2k-3)(2k-1)},$$

$$c_5 = \frac{3(k+3)(k+2)}{2(2k+5)(2k+3)},$$

$$c_{16} = \frac{-k^2(k-1)(k-3)}{2(2k-1)(2k-3)(2k+3)},$$

$$c_6 = \frac{-3(k-1)^2(k-2)}{(2k-1)(2k-3)},$$

$$c_{17} = \frac{(k+1)^2(k+2)(k+4)}{2(2k-1)(2k+5)(2k+3)},$$

$$c_7 = \frac{-3k(k+1)}{(2k-1)(2k+3)},$$

$$c_{18} = \frac{-3(k+3)^2(k+4)(k+2)}{2(2k+5)(2k+7)(2k+3)},$$

$$c_8 = \frac{3(k+2)^2(k+3)}{(2k+3)(2k+5)},$$

$$c_{19} = \frac{3(k-3)(k-2)(k-1)}{(2k-5)(2k-1)(2k-3)},$$

$$c_9 = \frac{-3(k+1)(k+2)(k+3)}{(2k+3)(2k+5)},$$

$$c_{20} = \frac{-3k^2(k-1)}{(2k-1)(2k-3)(2k+3)},$$

$$c_{10} = \frac{3(k-2)(k-1)k}{(2k-3)(2k-1)},$$

$$c_{21} = \frac{-3(k+1)^2(k+2)}{(2k+3)(2k-1)(2k+5)},$$

$$c_{11} = (k+1)^2 c_1,$$

$$c_{22} = \frac{-2}{k+3} c_{18}.$$